# DUAL ORDER PARAMETERS AND THE DECONFINEMENT TRANSITION*

Christian S. Fischer[a,b†] Jens A. Mueller[a‡]

[a]Institute for Nuclear Physics, Technische Universität Darmstadt
Schlossgartenstrasse 9, 64289 Darmstadt, Germany
[b]GSI Helmholtzzentrum für Schwerionenforschung GmbH,
Planckstrasse 1, 64291 Darmstadt, Germany

*(Received January 27, 2010)*

We investigate the chiral and the deconfinement transition within the framework of Dyson–Schwinger equations using quenched lattice data for the temperature dependent gluon propagator as input. We extract corresponding order parameters from the Landau gauge quark propagator with U(1)-valued boundary conditions. We study the chiral transition using the conventional quark condensate, whereas for the deconfinement transition we determine the dual condensate ('dressed Polyakov loop'). In addition, we consider an alternative order parameter for deconfinement, the dual scalar quark dressing function. As a result we find almost the same transition temperatures for the chiral and deconfinement transitions.

PACS numbers: 12.38.Aw, 12.38.Lg, 11.10.Wx

## 1. Introduction

The phases of QCD are currently under intense theoretical and experimental investigations. Open questions concern among others the interplay between the confinement/deconfinement transition and the chiral transition, *e.g.* the (non-)coincidence of the chiral and the deconfinement transition at zero chemical potential [1], and the possibility of a confined chirally symmetric ('quarkyonic') phase [2]. Answers to these questions certainly require non-perturbative approaches to QCD.

Functional methods involving the renormalization group equations [3] and/or Dyson–Schwinger equations (DSE) [4, 5] constitute a non-perturbative continuum approach to QCD. Only very recently, approaches ac-

* Talk presented at the EMMI Workshop and XXVI Max Born Symposium "Three Days of Strong Interactions", Wrocław, Poland, July 9–11, 2009.

† christian.fischer@physik.tu-darmstadt.de

‡ jens.mueller@physik.tu-darmstadt.de

counting also for the deconfinement transition became available for these methods [6–9]. These approaches allow to define order parameters for the deconfinement transition from the quark propagator for generalized boundary conditions. Originally introduced within the lattice framework [10,11] it was adapted to functional methods in [7–9]. The quantities calculated in this work signaling the deconfinement transition are the dual quark condensate (or 'dressed Polyakov loop') and the dual scalar quark dressing function.

In the following we first recall the defining equations for the ordinary and the dual quark condensate and scalar dressing function, then summarize the truncation scheme used in our DSE calculations before we discuss our results for the chiral and deconfinement phase transition.

## 2. Order parameters for deconfinement

Consider the full quark propagator at finite temperature given in terms of its Dirac structure by

$$S(\vec{p},\omega_p) = [i\Gamma_4\,\omega_p C(\vec{p},\omega_p) + i\Gamma_i\,p_i A(\vec{p},\omega_p) + B(\vec{p},\omega_p)]^{-1}\ , \qquad (1)$$

with vector dressing functions $A$ and $C$ and scalar dressing function $B$. The physical, antiperiodic boundary conditions in temporal direction lead to $\omega_p(n_t) = (2\pi T)(n_t + 1/2)$ for Matsubara frequencies. Generalizing to temporal U(1)-valued boundary conditions $\psi(\vec{x},1/T) = e^{i\varphi}\psi(\vec{x},0)$ results in Matsubara frequencies $\omega_p(n_t) = (2\pi T)(n_t + \varphi/2)$ with boundary angle $\varphi = [0, 2\pi[$.

From the $\varphi$-dependent propagator the dual quark condensate introduced in lattice gauge theory Ref. [11]

$$\Sigma_1 = \int_0^{2\pi} \frac{d\varphi}{2\pi}\, e^{-i\varphi}\, \langle\overline{\psi}\psi\rangle_\varphi \qquad (2)$$

can be calculated. Due to its close connection to the Polyakov loop it is also called 'dressed Polyakov loop', see Refs. [11,12] for more details.

The dual scalar quark dressing function introduced in Ref. [9] is the phase-Fourier-transform of the $\varphi$-dependent scalar quark dressing function evaluated at lowest Matsubara frequency and zero momentum

$$\Sigma_B = \int_0^{2\pi} \frac{d\varphi}{2\pi}\, e^{-i\varphi}\, B(0,\omega_p(0,\varphi))\,. \qquad (3)$$

Both quantities the dual quark condensate and the dual scalar quark dressing function transform under center symmetry identically as the conventional Polyakov loop and are therefore order parameters for deconfinement.

An advantage of the $\varphi$-dependent quark condensate $\langle\overline{\psi}\psi\rangle_\varphi$ is its direct connection to the ordinary Polyakov loop in the limit of static quarks [11]. For vanishing bare quark mass it is well-behaved in the continuum limit whereas at finite quark mass it is quadratically divergent and needs to be properly regularized. Though apparently not linked to the Polyakov loop the $\varphi$-dependent scalar quark dressing function $B(0,\omega_p(0,\varphi))$ has the advantage of being a well defined quantity also in the continuum limit.

## 3. The Dyson–Schwinger equation for the quark propagator at finite temperature

The Dyson–Schwinger equation for the quark propagator is displayed diagrammatically in Fig. 1. At finite temperature $T$ it is given by

$$S^{-1}(p) = Z_2 S_0^{-1}(p) - C_F Z_{1f} g^2 T \sum_{n_k} \int \frac{d^3k}{(2\pi)^3} \Gamma_\mu S(k) \Gamma_\nu(k,p) D_{\mu\nu}(p-k)\,, \quad (4)$$

with $p = (\vec{p}, \omega_p)$ and $k = (\vec{k}, \omega_k)$ and renormalization factors $Z_2$ and $Z_{1f}$. Here $D_{\mu\nu}$ denotes the (transverse) gluon propagator in Landau gauge and $\Gamma_\nu$ the quark–gluon vertex. The bare quark propagator is given by $S_0^{-1}(p) = i\Gamma\cdot p + m$. The Casimir factor $C_F = (N_c^2-1)/N_c$ stems from the color trace; here we only consider the gauge group SU(2). The quark dressing functions $A, B, C$ can be extracted from Eq. (4) by suitable projections in Dirac-space.

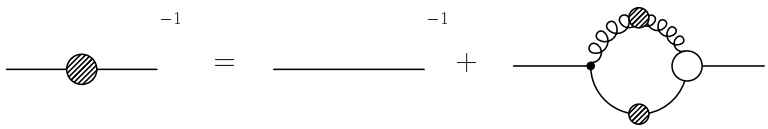


Fig. 1. The Dyson–Schwinger equation for the quark propagator. Filled circles denote dressed propagators whereas the empty circle stands for the dressed quark–gluon vertex.

In order to solve this equation we have to specify explicit expressions for the gluon propagator and the quark–gluon vertex. At finite temperatures the tensor structure of the gluon propagator contains two parts, one transversal and one longitudinal to the heat bath. The propagator is then given by ($q = (\vec{q}, \omega_q)$)

$$D_{\mu\nu}(q) = \frac{Z_{\mathrm{T}}(q)}{q^2} P^{\mathrm{T}}_{\mu\nu}(q) + \frac{Z_{\mathrm{L}}(q)}{q^2} P^{\mathrm{L}}_{\mu\nu}(q) \quad (5)$$

with transverse and longitudinal projectors

$$P^{\mathrm{T}}_{\mu\nu}(q) = \left(\delta_{ij} - \frac{q_i q_j}{\vec{q}^2}\right)\delta_{i\mu}\delta_{j\nu}\,, \qquad P^{\mathrm{L}}_{\mu\nu}(q) = P_{\mu\nu}(q) - P^{\mathrm{T}}_{\mu\nu}(q)\,, \tag{6}$$

with $(i,j = 1\ldots3)$. At zero temperatures Euclidean $O(4)$-invariance requires both dressing functions to agree, *i.e.* $Z_{\mathrm{T}}(q) = Z_{\mathrm{L}}(q) = Z(q)$.

The temperature dependence of the gluon propagator can be inferred from recent lattice calculations. The results of Ref. [13] are shown in Fig. 2. The lattice data although still with quantitative uncertainties may very well correctly represent the qualitative temperature dependence of the gluon propagator. We therefore use a temperature dependent (qualitative) fit to the data as input into the DSE; this fit is also displayed in Fig. 2 (straight lines). The fit functions are described in detail in Refs. [8, 9] and shall not be repeated here for brevity. Note, however, that we also inherit the scale determined on the lattice using the string tension $\sqrt{\sigma} = 0.44$ GeV [13].

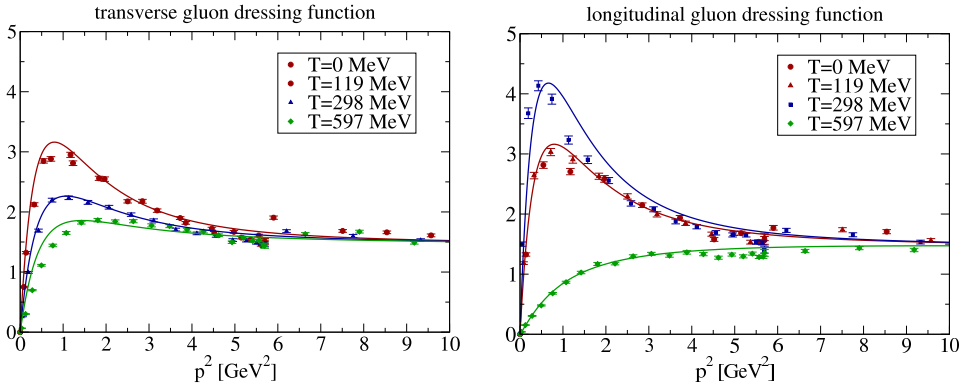


Fig. 2. Quenched SU(2) lattice results [13] for the transverse dressing function $Z_{\mathrm{T}}(q)$ and the longitudinal dressing function $Z_{\mathrm{L}}(q)$ of the gluon propagator together with the fit functions [8].

For the quark–gluon vertex we employ a temperature dependent model which is discussed in detail in [9].

## 4. Numerical results

In Fig. 3 we display our numerical results for the ordinary and the dual quark condensate together with their (normalized) temperature derivatives once evaluated for a quark mass of $m = 10$ MeV (fixed at $T = 200$ MeV and $\vec{\mu}^2 = 20$ GeV$^2$) and once evaluated in the chiral limit. One clearly sees the difference in the chiral transition: whereas at finite bare quark mass

we encounter a crossover the transition changes into a second order phase transition in the chiral limit. In the first case the corresponding temperature derivative shows a peak at $T_c = 301(2)$ MeV, whereas it diverges at $T_c = 298(1)$ MeV in the second case. We also extracted the corresponding transition temperatures from the chiral susceptibility

$$\chi_R = m^2 \frac{\partial}{\partial m} \Big( \langle \bar{\psi}\psi \rangle_T - \langle \bar{\psi}\psi \rangle_{T=0} \Big) . \tag{7}$$

The results for quark mass $m = 10$ MeV are given in Table I.

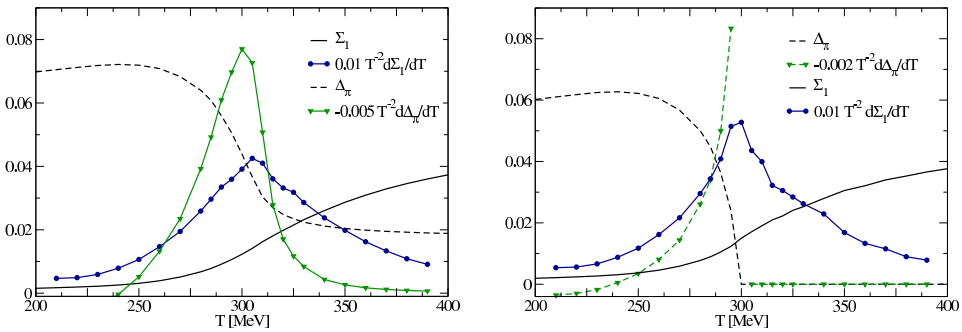


Fig. 3. Left diagram: Temperature dependence of the dressed Polyakov loop $\Sigma_1$ and the conventional quark condensate $\Delta_\pi \equiv \langle \overline{\psi}\psi \rangle_{\varphi=\pi}$ together with their derivatives for $m = 10$ MeV. Right diagram: The same quantities in the chiral limit.

TABLE I

Transition temperatures for the chiral and deconfinement transition for quark mass $m = 10$ MeV.

| $T_c$ | $T_{\chi_R/T^4}$ | $T_{\chi_R}$ | $T_{dec}$ |
|---|---|---|---|
| 301(2) | 304(1) | 305(1) | 308(2) |

The corresponding transition temperature for the deconfinement transition can be read off the dual quark condensate (or dressed Polyakov loop). At finite quark mass and in the chiral limit we observe a distinct rise in the dual condensate around $T \approx 300$ MeV. The corresponding (normalized) temperature derivative shows a peak at $T_{dec} = 308(2)$ MeV for quark mass $m = 10$ MeV. In the chiral limit this peak moves to $T_{dec} = 299(3)$ MeV.

In general we note that the chiral and deconfinement transition are close together. There are a few MeV difference between the different transition temperatures for the crossover at finite quark masses, whereas both transitions occur at the same temperature (within errors) in the chiral limit. These findings agree with early expectations from lattice simulations [14].

Furthermore we wish to emphasize that the present calculation, although carried out with quenched lattice results for the gluon propagator, is in itself not strictly quenched. This can be seen from the fact that the dressed Polyakov loop is not strictly zero below the deconfinement transition. We refer here to quenched calculation since the influence of the matter content to the gauge sector is neglected.

In the left diagram of Fig. 4 we show a comparison of the dual scalar dressing Eq. (3) with the dual condensate for $m = 10$ MeV. Both quantities show a very similar temperature dependence especially the aforementioned distinct rise around $T \approx 300$ MeV. The signal is slightly stronger for the dual scalar dressing $\Sigma_B$. The temperature derivatives indicating the deconfinement transition clearly peak at the same transition temperature.

In the plot of the right hand side of Fig. 4 the chiral condensate $\langle\bar{\psi}\psi\rangle_{\varphi=0}$ and the quark scalar dressing $B(\varphi = 0)$ as functions of temperature at periodic boundary conditions are shown. For comparison both are normalized to 1 at $T = 500$ MeV. Whereas $\langle\bar{\psi}\psi\rangle_{\varphi=0}$ is a strictly monotonic function with temperature the scalar dressing is slightly decreasing in the temperature range between 300 and 400 MeV before the high temperature behavior shows up. The large temperature scaling of both quantities can be extracted analytically from Eqs. (2) and (4) as pointed out in the appendix of Ref. [9]. There it is shown that

$$B_{\varphi=0,\ p=0}(T) \sim \sqrt{T}\,, \qquad \text{for } T \gg T_{\rm c} \tag{8}$$

and consequently a quadratic rise of the condensate,

$$\langle\bar{\psi}\psi\rangle_{\varphi=0} \sim T^2\,, \qquad \text{for } T \gg T_{\rm c}\,, \tag{9}$$

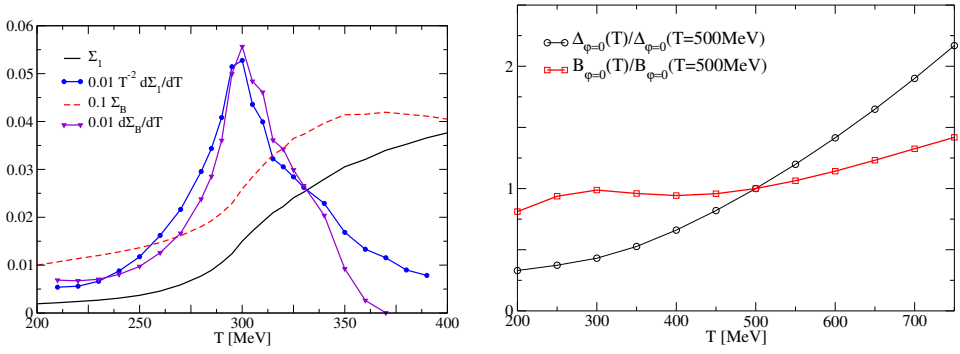


Fig. 4. Left diagram: Comparison of the temperature dependence of the corresponding dual scalar quark dressing and the dual condensate for $m = 10$ MeV. Right diagram: Temperature dependence of the chiral quark condensate $\Delta_\varphi \equiv \langle\bar{\psi}\psi\rangle_\varphi$ and the scalar dressing function $B_\varphi$ at periodic boundary conditions $\varphi = 0$.

is obtained. These results are in excellent agreement with polynomial fits to the data. The dual condensate $\Sigma_1$ as well as the dual scalar dressing $\Sigma_B$ are promising candidates for a further study of the deconfinement transition of QCD.

## 5. Summary

In this paper we addressed the chiral and the deconfinement transition of quenched QCD. We showed results for the order parameter of the chiral transition, the quark condensate, and for order parameters of the deconfinement transition, the dressed Polyakov loop and the dual scalar dressing. These were extracted from the Landau gauge quark propagator evaluated at a continuous range of boundary conditions for the quark fields. Independent of the dual order parameter used we found exactly the same deconfinement transition temperature. A comparison of the transition temperatures for the chiral and the deconfinement transition shows almost coincidence for moderate quark mass of the order of an up-quark. In the chiral limit the two transitions coincide within error. We find a second order chiral phase transition at $T_{\chi_R/T^4} = 298(1)$ MeV and a similar temperature for the deconfinement transition, $T_{\rm dec} = 299(3)$ MeV. In summary, we conclude that the chiral and deconfinement transition temperatures are only slightly different for finite quark masses and coincide within errors in the chiral limit.

The framework used in this work is quenched SU(2) Yang-Mills theory. Our transition temperature may be translated into the corresponding ones of quenched SU(3) QCD using the relations $T_c/\sqrt{\sigma} = 0.709$ (SU(2)) and $T_c/\sqrt{\sigma} = 0.646$ (SU(3)) between the respective critical temperatures and the string tension [16]. The resulting transition temperature is then $T_{\chi_R/T^4} \approx T_{\rm dec} \approx 272$ MeV in the chiral limit. In order to work in the full, unquenched theory quark loop effects and meson effects which shift the transition temperature below $T = 200$ MeV have to be taken into account. Concerning the dual condensate and scalar dressing function in the unquenched formulation additional effects due to the Roberge–Weiss symmetry [15] occur. This is because of the formal similarity of the continuous boundary conditions for the quark field to an imaginary chemical potential, see [6] for details.

It is a pleasure to thank the organizers of this exciting and inspiring workshop for their efforts. This work has been supported by the Helmholtz University Young Investigator Grant VH-NG-332 and by the Helmholtz Alliance HA216-TUD/EMMI.

## REFERENCES


[1] A. Bazavov *et al.*, *Phys. Rev.* **D80**, 014504 (2009) [arXiv:0903.4379[hep-lat]]; Y. Aoki *et al.*, *J. High Energy Phys.* **0906**, 088 (2009) [arXiv:0903.4155[hep-lat]].

[2] L. McLerran, R.D. Pisarski, *Nucl. Phys.* **A796**, 83 (2007) [arXiv:0706.2191[hep-ph]]; L. McLerran, K. Redlich, C. Sasaki, *Nucl. Phys.* **A824**, 86 (2009) [arXiv:0812.3585[hep-ph]].

[3] J. Berges, N. Tetradis, C. Wetterich, *Phys. Rep.* **363**, 223 (2002) [arXiv:hep-ph/0005122]; H. Gies, arXiv:hep-ph/0611146.

[4] C.D. Roberts, S.M. Schmidt, *Prog. Part. Nucl. Phys.* **45**, S1 (2000) [arXiv:nucl-th/0005064].

[5] C.S. Fischer, *J. Phys. G* **32**, R253 (2006) [arXiv:hep-ph/0605173].

[6] F. Marhauser, J.M. Pawlowski, arXiv:0812.1144[hep-ph].

[7] J. Braun, L. Haas, F. Marhauser, J.M. Pawlowski, arXiv:0908.0008[hep-ph].

[8] C.S. Fischer, *Phys. Rev. Lett.* **103**, 052003 (2009) [arXiv:0904.2700[hep-ph]].

[9] C.S. Fischer, J.A. Mueller, *Phys. Rev.* **D80**, 074029 (2009) [arXiv:0908.0007[hep-ph]]; arXiv:0908.2530[hep-ph].

[10] C. Gattringer, *Phys. Rev. Lett.* **97**, 032003 (2006) [arXiv:hep-lat/0605018].

[11] E. Bilgici, F. Bruckmann, C. Gattringer, C. Hagen, *Phys. Rev.* **D77**, 094007 (2008) [arXiv:0801.4051[hep-lat]].

[12] F. Synatschke, A. Wipf, K. Langfeld, *Phys. Rev.* **D77**, 114018 (2008) [arXiv:0803.0271[hep-lat]].

[13] A. Cucchieri, A. Maas, T. Mendes, *Phys. Rev.* **D75**, 076003 (2007) [arXiv:hep-lat/0702022].

[14] F. Karsch, arXiv:hep-lat/9903031.

[15] A. Roberge, N. Weiss, *Nucl. Phys.* **B275**, 734 (1986).

[16] J. Fingberg, U.M. Heller, F. Karsch, *Nucl. Phys.* **B392**, 493 (1993) [arXiv:hep-lat/9208012]; O. Kaczmarek, F. Karsch, P. Petreczky, F. Zantow, *Phys. Lett.* **B543**, 41 (2002); [arXiv:hep-lat/0207002]; B. Lucini, M. Teper, U. Wenger, *J. High Energy Phys.* **0502**, 033 (2005) [arXiv:hep-lat/0502003].

[17] K. Kashiwa, H. Kouno, M. Yahiro, *Phys. Rev.* **D80**, 117901 (2009) [arXiv:0908.1213[hep-ph]].